Efficient Channel Delay Estimation for OFDM Systems over Doubly-Selective Fading Channels

Seo Weon Heo [1] and Jongtae Lim[1]
[1] School of Electronic & Electrical Eng., Hongik University
Seoul, Korea 121-791
[e-mail: {seoweon.heo, jlim}@hongik.ac.kr]
*Corresponding author: Jongtae Lim

Received January 11, 2012; revised May 17, 2012; accepted September 12, 2012; published September 26, 2012

Abstract

In this paper, we propose an efficient channel delay estimation method for orthogonal frequency-division multiplexing (OFDM) systems, especially over doubly-selective fading channels which are selective in both the symbol time domain and subcarrier frequency domain. For the doubly-selective fading channels in single frequency network (SFN), long and strong echoes exist and thus the conventional discrete Fourier Transform (DFT) based channel delay estimation system often fails to produce the exact channel delay profile. Based on the analysis of the discrete-time frequency response of the channel impulse response (CIR) coefficients in the DFT-based channel delay estimation system, we develop a method to effectively extract the true CIR from the aliased signals by employing a simple narrow-band low-pass filter (NB-LPF). The performance of the proposed system is verified using the COST207 TU6 SFN channel model.

Keywords: OFDM, channel delay estimation, doubly-selective fading channel, single frequency network, channel impulse response

This research was supported in part by the Basic Science Research Program through the National Research Foundation of Korea (NRF) funded by the Ministry of Education, Science and Technology (NRF-2012-0001368)
http://dx.doi.org/10.3837/tiis.2012.09.014

1. Introduction

Orthogonal Frequency-Division Multiplexing (OFDM) has been widely deployed in various wireless communication applications such as digital broadcasting, mobile communications and wireless networks [1][2][3]. One of the main reasons for adopting OFDM is the robustness to multi-path fading and easiness of channel equalization. However, for fast-fading channels where the channel is not time-invariant within one OFDM symbol, OFDM systems have some performance degradation due to the random amplitude attenuation of the received signals and inter-carrier interference (ICI) caused by the Doppler spreading. Many diversity techniques in the transmitter or receiver side have been studied to solve the problem caused by the randomly attenuated signals [4][5]. The ICI mitigation problem has been investigated in many research works [3][5][6][7][8].

To mitigate the effect caused by ICI, the estimation of channel characteristics is considered as one of the most important issues. In the channel estimation for fast-fading channels, many parameters need to be estimated, unlike for slowly time-varying channels where ICI is negligible. To reduce the number of the channel parameters to be estimated, some approaches based on the basis expansion model (BEM) have been proposed in [9][10]. The BEM algorithm reduces the required number of channel parameters by assuming that the channel can be represented by a number of basis functions. Thus, the estimation of the number of the basis functions is the very first parameter to estimate in the BEM approaches. For this purpose, the channel delay parameters should be accurately evaluated to get a reliable estimate of the number of basis functions.

Another approach to reducing the number of channel parameters has been proposed on the assumption that the channel condition varies linearly during one OFDM symbol time duration [7]. Whereas the algorithm has several limitations due to the linearity assumption, it is attractive in the sense that the structure is easy to implement in very large scale integration (VLSI). Its simple implementation is due to the fact that the channel estimation is performed with only the channel frequency response, which is obtained by the conventional methods using either a simple least square estimator combined with interpolation filtering or transform domain methods using the discrete Fourier transform (DFT). In addition, the other channel parameters such as ICI channel gains can be estimated using the conventional channel estimation algorithm with a simple linear interpolation.

However, the conventional channel estimation algorithms do not perform well when the rate of channel variation is high. This degradation becomes severe especially when the receiver operates in single frequency network (SFN) where the delay profile can be very large. In this case, the channel impulse response (CIR) which is obtained during the conventional channel estimation processing is corrupted by the aliasing effect in the frequency domain and thus fails to get a good estimate of the channel delay. This is usually caused by the sparsity of the distributive pilot subcarrier locations which is intentionally inserted for channel estimation in most OFDM systems. Although the pilot subcarrier patterns are different with OFDM systems, most systems locate the pilot subcarriers in an OFDM symbol at some offset distance from the previous symbol. For example, the pilot subcarriers are located at three subcarriers apart from the previous OFDM symbol in digital video broadcasting-terrestrial (DVB-T) and integrated services digital broadcasting-terrestrial (ISDB-T) systems. In this paper, we propose a simple and efficient method to estimate the channel delay parameters for doubly-selective fading channels in SFN. Based on the analysis that the pilot subcarrier offset

causes the pseudo CIR components, i.e., the false CIR components due the aliasing effect, which take different center frequency in the frequency domain, we develop a simple channel delay estimation algorithm using a narrow-band low-pass filter (NB-LPF) and pseudo CIR removal circuits.

The rest of this paper is organized as follows. Section 2 describes the OFDM systems and the conventional discrete Fourier transform (DFT)-based channel delay estimator. The frequency domain characteristics of the CIR coefficient are analyzed in Section 3. Section 4 introduces the proposed channel delay estimation algorithm. The performance of the proposed system is verified in Section 5 under the well-known COST 207 TU6 SFN channel model for DVB-T systems. Finally, we conclude the paper in Section 6.

2. System Description

The basic block diagram of a general OFDM transmission system is shown in **Fig. 1**. Prior to the modulation, the transmitted data bits are encoded by a channel encoder and are interleaved by a bit-interleaver. The coded and interleaved bits are mapped into the constellation points to obtain data symbols. The serial data symbols are then converted to parallel data symbols. On the data symbols, the pilot subcarriers are added at the pre-defined locations. Then, the inverse fast Fourier transform (IFFT) is performed to obtain time-domain OFDM symbols. The OFDM symbols are extended by inserting cyclic prefix (CP) and followed by the parallel-to-serial converter. The converted symbols are transmitted over the channel.

At the receiver, CP is removed from the received signal and the signal is transformed to frequency domain by the fast Fourier transform (FFT). After processing the channel estimation, the frequency domain signal is converted to serial data symbols and the data symbols are demodulated to reproduce the transmitted information bits using deinterleaving and channel decoding.

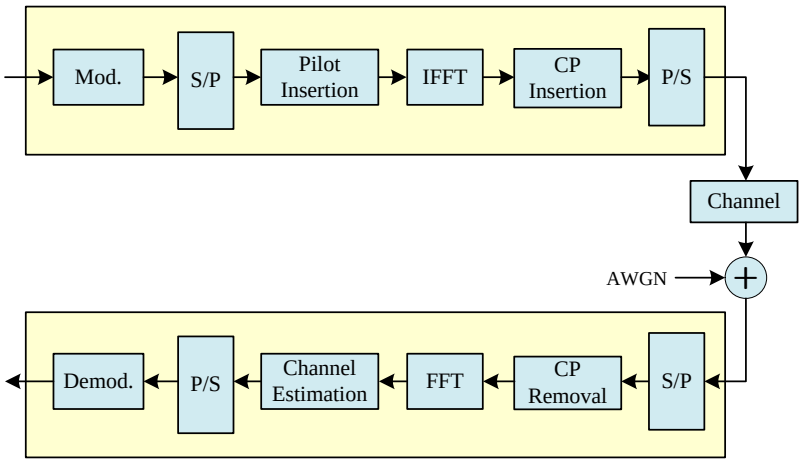

Fig. 1. Block diagram of a general OFDM transmission system

To recover the transmitted information bits, the receiver needs to estimate and compensate the channel frequency response (CFR). For this purpose, the OFDM system inserts pilot tones at the regularly distributed subcarrier positions as shown in **Fig. 2**. The distance between two adjacent pilot subcarriers in an OFDM symbol is denoted as D_s, the difference of the pilot

offsets of two adjacent OFDM symbols as D_o, and the period during which the same pilot pattern repeats as D_p.

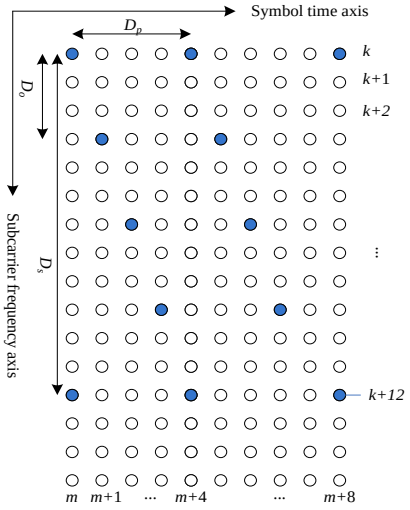

Fig. 2. Distributed pilot patterns in an OFDM symbol

The transmitted signal at the m^{th} OFDM symbol in the CIR time domain is expressed as

$$x(m,n)=\frac{1}{N}\sum_{k=0}^{N-1}X(m,k)e^{j\frac{2\pi kn}{N}}, \qquad k=0,\cdots,N-1, \tag{1}$$

where $X(m,k)$ is the frequency domain signal of a k^{th} subcarrier at m^{th} OFDM symbol and N is the number of total subcarriers. Channel characteristics in the continuous time domain can be described by

$$h(t,\tau)=\sum_{l=0}^{L-1}\alpha_l(t)\delta(\tau-\tau_l), \tag{2}$$

where L is the number of multi-paths, $\alpha_l(t)$ denote the channel gain coefficient and τ_l denotes the time delay for the l^{th} multi-path. Using the tapped delay-line channel model, the channel in the discrete time domain is represented as

$$h^{(n)}(m,u)=\sum_{l=0}^{L-1}\alpha_l(m,n)\delta(u-u_l), \qquad 0\le n,u\le N-1, \tag{3}$$

where $\alpha_l(m,u)$ and u_l denote the time varying channel gain coefficient and time delay of m^{th} OFDM symbol at time n, respectively. Then the received signal through the channel and AWGN addition can be expressed as

$$y(m,n)=\sum_{u=0}^{N-1}h^{(n)}(m,u)x\left(m,(n-u)_N\right)+w(m,n), \tag{4}$$

where $()_N$ represents a cyclic shift in the base of N and $w(m,n)$ is the AWGN.

Assuming perfect time and frequency synchronization, the received signal after DFT transform can be written as [7]

$$\begin{aligned} Y(m,k)&=H(m,k)X(m,k)+\sum_{u=0,u\neq k}^{N-1}H_{ICI}(m,u,k)X(m,u)+W(m,k)\\ &=H(m,k)X(m,k)+X_{ICI}(m,k)+W(m,k), \end{aligned} \tag{5}$$

where $H(m,k)$ is the CFR at the k^{th} subcarrier given by

$$H(m,k)=\sum_{l=0}^{L-1}\left\{\frac{1}{N}\sum_{n=0}^{N-1}\alpha_l(m,n)\right\}e^{-j\frac{2\pi kn_l}{N}}=DFT_n\left\{h^{ave}(m,n)\right\}, \tag{6}$$

$H_{ICI}(m,u,k)$ is the multiplicative ICI channel parameters contributed by the u^{th} subcarrier onto the k^{th} subcarrier at the symbol time m, and $W(m,k)$ is the DFT of the AWGN signal. Notice that $H(m,k)$ is the DFT of the time averaged CIR in an OFDM symbol.

The estimation of the channel delays n_l's is performed using the DFT-based channel delay estimator shown in **Fig. 3**.

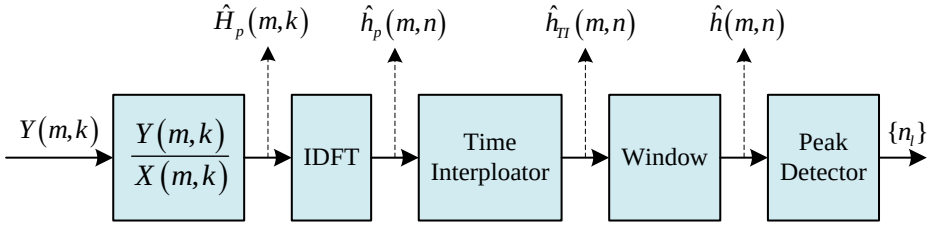

Fig. 3. Block diagram of the DFT-based channel delay estimator

Using the widely-adopted least square method, the CFR at the pilot positions is estimated as

$$\hat{H}_p(m,k)=\frac{Y(m,k)}{X(m,k)}\cdot\sum_{k'=0}^{N_p-1}\delta\left(k-\left(m_pD_o+k'D_s\right)\right)=\hat{H}_a(m,k)\cdot D(m,k), \tag{7}$$

where $\delta(k)$ is the Kronecker delta function, N_p is the number of pilot tones in an OFDM symbol, m_p is (m mod D_p) and $D(m,k)$ is $\sum_{k'=0}^{N_p-1}\delta\left(k-\left(m_pD_o+k'D_s\right)\right)$. The delta function is used to represent the pilot patterns in 2-dimensional space, i.e., subcarrier frequency domain and

symbol time domain. Then time-domain interpolation filtering is performed and the CFR is given by

$$\hat{H}_{TI}(m,k)=\sum_{u=-(D_p-1)}^{D_p-1}\hat{H}_p(m-u,k)F_{lin}(u), \tag{8}$$

where $F_{lin}(u)$ is the time-domain interpolation filter. A typical example of the filter is the linear interpolation filter given by

$$F_{lin}(u)=\begin{cases}\dfrac{D_p-|u|}{D_p}, & 0\le|u|\le D_p-1\\ 0, & otherwise\end{cases}. \tag{9}$$

After the time-domain interpolation filtering, the channel impulse response in the (CIR) time domain is obtained by the IDFT. Then, the peak detection algorithm is applied to separate each channel delay parameters n_l's, $l=1,\cdots,L-1$. Notice that the position of IDFT and time-domain interpolation filtering is interchanged in **Fig. 3** to ease the explanation in the next Section. Since both operations are linear, this interchange does not affect the overall estimation operation.

3. Frequency Domain Characteristics Of CIR

The channel impulse response for the m^{th} OFDM symbol is obtained from (7) by

$$\begin{aligned}\hat{h}_p(m,n)&=IDFT_k\left\{\hat{H}_p(m,k)\right\}=IDFT_k\left\{\hat{H}_a(m,k)D(m,k)\right\}\\&=\sum_{u=0}^{N-1}\hat{h}_a\left(m,(n-u)_N\right)d(m,u),\end{aligned} \tag{10}$$

where

$$d(m,n)=IDFT_k\left\{D(m,k)\right\}=\frac{1}{N}\sum_{k'=0}^{\lfloor N/D_s\rfloor-1}e^{-j\frac{2\pi(mD_o+k'D_s)n}{N}}. \tag{11}$$

For simplicity, N is assumed to be a multiple of D_s. If N is not a multiple of D_s, more elaborate equations need to be evaluated but the overall analysis remains unchanged. Then (11) is expressed as

$$d(m,n)=\frac{1}{N}\sum_{k'=0}^{N/D_s-1}e^{-j\frac{2\pi(mD_o+k'D_s)n}{N}}=\sum_{n'=0}^{D_s-1}\left\{e^{-j\frac{2\pi mD_o n'}{N}}\cdot\delta\left(n-n'\frac{N}{D_s}\right)\right\} \tag{12}$$

and the channel impulse response given by (10) becomes

$$\begin{aligned}\hat{h}_p(m,n) &= \sum_{u=0}^{N-1}\hat{h}_a\left(m,(n-u)_N\right)\sum_{n'=0}^{D_s-1}\left\{e^{-j\frac{2\pi mD_o n'}{N}}\cdot\delta\left(u-n'\frac{N}{D_s}\right)\right\} \\ &= \sum_{n'=0}^{D_s-1}\left\{e^{-j\frac{2\pi mD_o n'}{N}}\cdot\hat{h}_a\left(m,n-n'\frac{N}{D_s}\right)\right\}.\end{aligned} \tag{13}$$

Notice that only the first term for $n'=0$ in (13) corresponds to the true CIR, and all the other D_s-1 terms are image signals caused by the pilot patterns in the subcarrier frequency domain.

To investigate the frequency domain characteristics of the CIR, the discrete-time Fourier transform (DTFT) of $\hat{h}_p(m,n)$ is calculated as

$$\begin{aligned}\hat{G}_p(\omega,n) &= DTFT_m\left\{\hat{h}_p(m,n)\right\} \\ &= \sum_{n'=0}^{D_s-1}DTFT_m\left\{e^{-j\frac{2\pi mD_o n'}{N}}\cdot\hat{h}_a\left(m,n-n'\frac{N}{D_s}\right)\right\} \\ &= \sum_{n'=0}^{D_s-1}\hat{G}_a\left(\omega-\left(\frac{2\pi mD_o}{N}\right)n',n-n'\frac{N}{D_s}\right),\end{aligned} \tag{14}$$

where $\hat{G}_a(\omega,n)$ is the DTFT of the time-domain CIR estimate $\hat{h}_a(m,n)$. In (14), it is important to note that the spectrum of the CIR consists of the component which is corresponding to the true CIR and the components of the true CIR's repetition patterns that occupy different center frequencies in the frequency domain. This is the key observation we will use for the estimation of channel delay parameters. Depending on the aliasing of these components, the performance of channel delay estimation varies greatly.

To see the effect of the aliasing on the estimation performance, we evaluate the frequency response of the CIR for the slow and fast moving receivers in a SFN. For the evaluation, one TU6 channel with the time delay 0 and the other TU6 channel with the time delay 180μs are taken, and 50 km/h and 200 km/h are chosen as the speed of the slow and fast moving receivers, respectively. **Fig. 4** shows the magnitude of DTFT of the first four CIR components when the receiver is moving at relatively low speed (50km/h). Since the maximum Doppler frequency is not high, the spectrum of the CIRs do not overlap each other. Thus, after the time-domain interpolation filtering, the peak detection algorithm is successfully performed and produces the peakes corresponding to only the true CIR as shown in **Fig. 5**. On the other hand, for the fast moving receiver, the maximum Doppler frequency becomes higher and thus the spectrum of the CIR components overlaps as shown in **Fig. 6**. Thus, the same peak detection algorithm cannot produce reliable channel delay estimation and has several peaks that are not corresponding to the true CIR as shown in **Fig. 7**. Therefore, more sophisticated channel delay algorithm needs to be developed to mitigate the effect of the overlaps for the fast moving receivers.

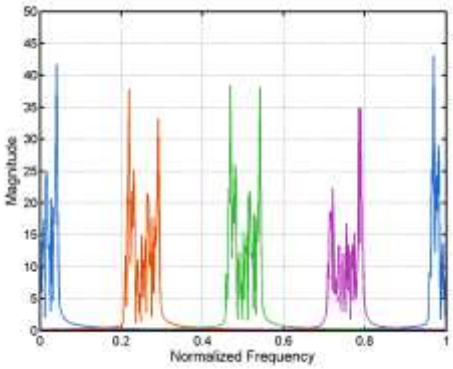

Fig. 4. Spectrum of the CIR for slow moving receiver

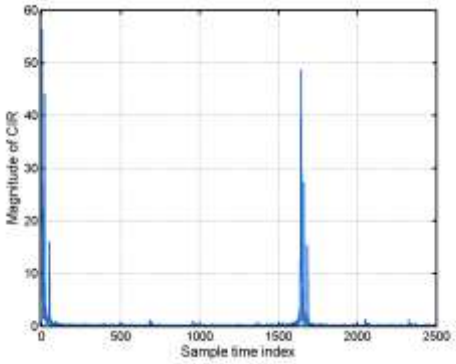

Fig. 5. CIR after interpolation filtering for slow moving receiver

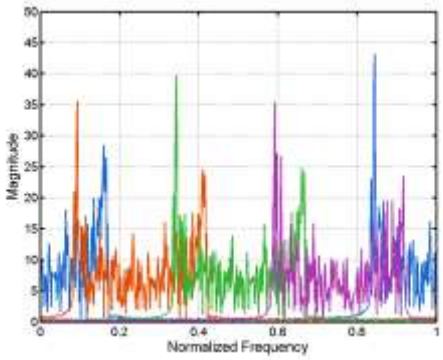

Fig. 6. Spectrum of the CIR for fast moving receiver

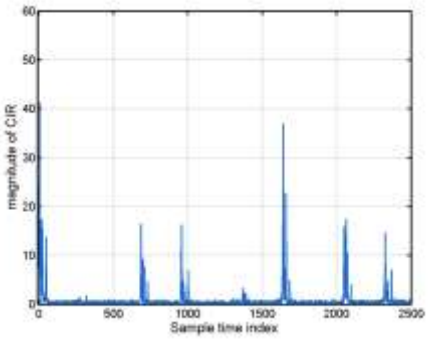

Fig. 7. CIR after interpolation filtering for fast moving receiver

4. CHANNEL DELAY ESTIMATION USING NB-LPF

To overcome the performance degradation of channel delay estimation due to the overlap of the CIR components in the conventional DFT-based channel delay estimator, we propose an efficient channel delay estimation method employing a narrow-band low-pass filter (NB-LPF), which is described in **Fig. 8**. As shown in the figure, the proposed channel delay estimator consists of the DFT-based channel delay estimator with a NB-LPF and a pseudo delay remover. The difference between the conventional DFT-based channel delay estimation and the proposed system is that the proposed system uses the NB-LPF to remove the pseudo channel delay occurred by the aliasing of the CIR components before performing the peak detection. As discussed in the previous section, the spectrum of the true CIR and all the other image signals occupy different center frequencies. Furthermore, most of the energy components around the low frequency region are from the true CIR as shown in **Fig. 6**. Applying the NB-LPF, the CIR corresponding to the true CIR component is extracted and processed by the peak detector.

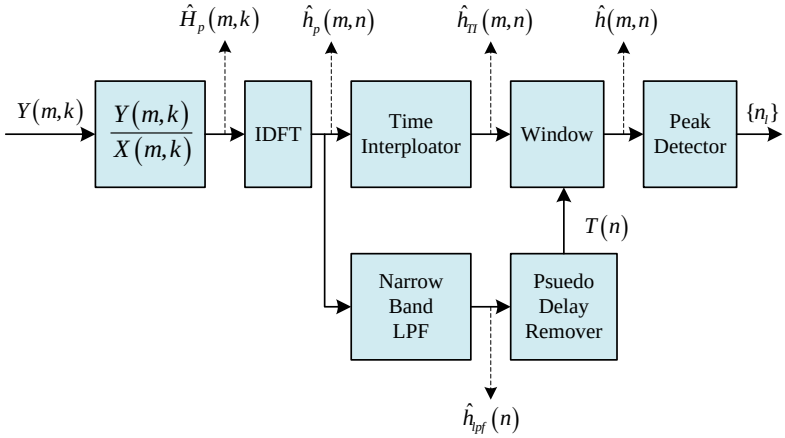

Fig. 8. Proposed channel delay estimator

Though the amplitude and phase of the CIR change rapidly in fast fading channels, the delay profile does not change rapidly. Thus, a simple short-tap infinite impulse response (IIR) LPF

can be used as the NB-LPF in the proposed estimator. The impulse response of the NB-LPF can be described by

$$\hat{h}_{lpf}(k) = \sum_{l} a_l \hat{h}_{lpf}(k-l) + \sum_{m} b_m \cdot \hat{h}_p(m, k-l) \ , \tag{15}$$

where $\{a_l\}$ and $\{b_m\}$ are the filter coefficients. In the proposed system, the bandwidth of the NB-LPF is much smaller than that of the time-domain interpolation filter to efficiently remove the frequency components caused by the adjacent pseudo CIR components. In **Fig. 9**, we show the magnitude spectrum of the IIR filter used in the simulation. The designed filter is a 4^{th}-order Chebyshev filter with cutoff frequency 0.1 in the normalized frequency domain.

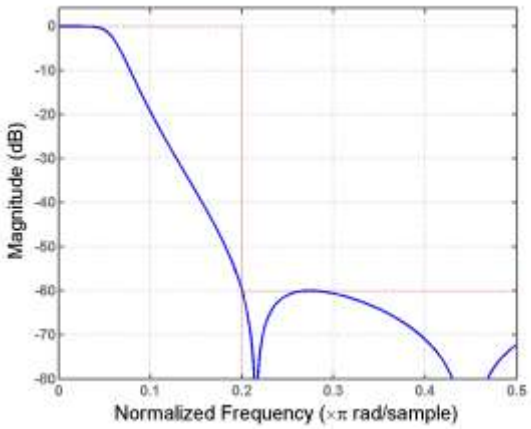

Fig. 9. Magintude response of the designed IIR filter.

After the lowpass filtering, the energy of the LPF output is measured and then the decision is performed to determine whether the n^{th} impulse response is corresponding to the true multi-path or the pseudo multi-path by the following threshold test:

$$T(n) = \begin{cases} 1, & if \quad f\left(\hat{h}_{lpf}(n)\right) > C_{th} \\ 0, & otherwise \end{cases}, \tag{16}$$

where $f(x)$ is a function that produce decision variables to be compared with some fixed or adaptive threshold constant C_{th}. In this paper, $f(x)$ is selected as the function that produces the absolute value of x, i.e., $f(x) = |x|$.

5. Simulation Results

For the simulation of the proposed channel delay estimator, we consider the DVB-T transmission system. The system parameters used in this simulation are listed in **Table 1**. The mobile speed is set to 200 *km*/*h* for considering the fast moving receiver.

Table 1. System Parameters

Parameters	Value
FFT size	8192
Number of sub-carriers	6817
OFDM symbol duration (T_u)	896 μs
Guard interval / T_u	1/4
Carrier frequency	800 *MHz*

The channel is modeled with the COST 207 which describes typical channel characteristics for the transmit bandwidth of 10 ~ 20 *MHz* around 900 *MHz* GSM band. Especially the TU-6 channel is selected, which is the terrestrial propagation model in an urban area. The TU-6 channel uses 6 resolvable paths whose delay and power profiles are listed in **Table 2**. In our simulation, we use the tapped delay-line (TDL) channel model whose tap positions approximate the delay profile of TU6. For the simulation of a SFN, another copy of the bottom profile is added at the starting delay position of 180 μs. This is a typical channel model for the SFN test scenario in DVB-T system.

Table 2. Characteristics of COST 207 TU-6 channel

Delay (μs)	Power (*dB*)	Fading Model
0.0	-3	Rayleigh
0.2	0	Rayleigh
0.5	-2	Rayleigh
1.6	-6	Rayleigh
2.3	-8	Rayleigh
5.0	-10	Rayleigh

Fig. 10 shows the magnitude of the NB-LPF output signal of the proposed channel delay estimation system. It is noticeable that the pseudo CIR components caused by the aliasing are effectively removed by the NB-LPF in the proposed system. The true CIR indication function $T(k)$ is shown in **Fig. 11**, which shows that the true channel delay can be extracted by the proposed channel delay estimator of OFDM systems over doubly-selective fading channels.

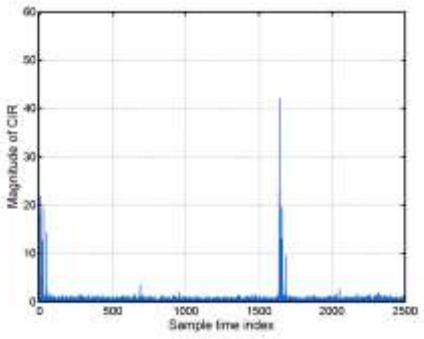

Fig. 10. Magnitude of the output signal of NB- LPF in the proposed system

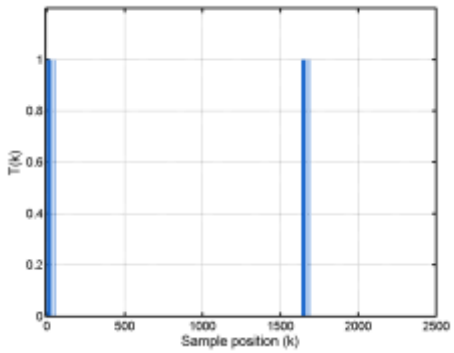

Fig. 11. true CIR indication function $T(k)$

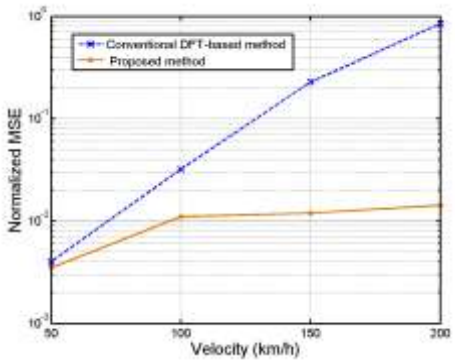

Fig. 12. Normalized MSE of the proposed and conventional method

To show the reliablility of the proposed channel delay estimation method, we compare the performance of the proposed method with the conventional DFT-based method. **Fig. 12** shows the normalized mean square error (NMSE) performance of two estimation methods, where the SNR is set to 20 dB and the mobile velocities are in the range of 50 km/h and 200 km/h. For the low velocity, maximum Doppler frequency is not high, thus the performance difference of the proposed and conventional methods is not significant. However, as the mobile speed becomes higher, the performance gap of two methods increases significantly. Moreover, the proposed method shows more stable performance for higher velocities, whereas the NMSE of the conventional method increases in propotion to the mobile velocity. This shows that the proposed method effectively separate and remove the pseudo CIR caused by the aliasing effect.

6. Conclusion

An efficient channel delay estimation algorithm is proposed for OFDM systems over doubly-selective fading channels. Based on the observations of the frequency characteristics of the CIR coefficients, a method for channel delay estimation is devised to extract the necessary true CIR from the aliased signal in the frequency domain using a simple narrow-band LPF. With the typical channel model for a SFN test scenarios of DBV-T systems the performance of the proposed system is evaluated and verified. The proposed algorithm

does not require complex operations and thus it can be easily implemented in very large scale integration (VLSI). More research on the determination of the proper threshold for the true CIR indication function and its performance analysis needs to be investigated in the future work.

References

[1] J. Zhou, Z. Ou, M. Rautianinen, T. Koskela and M. Ylianttila, "Digital television for mobile devices," *IEEE Multimedia*, vol.16, no.1, pp.60-71, Jan.2009. Article (CrossRef Link).

[2] U. Ladebusch and C. A. Liss, "Terrestrial DVB (DVB-T): A broadcast technology for stationary portable and mobile use," in *Proc. of IEEE*, vol.94, no.1, pp.183-193, Jan.2006. Article (CrossRef Link).

[3] K. Kwak, S. Lee, H. Min, S. Choi and D. Hong, "New OFDM channel estimation with dual-ICI cancellation in highly mobile channel", *IEEE Transactions Wireless Commuunication*, vol.9, no.10, pp.3155-3165, Oct.2010. Article (CrossRef Link).

[4] L. Vangelista et al.,"Key technologies for next-generation terrestrial digital television standard DVB-T2," *IEEE Communication Mag.*, vol.47, no.10, pp.146-153, 2009. Article (CrossRef Link).

[5] D. Gozalvez, D. Gomez-Barquero, D. Vargas and N. Cardonam, "Time diversity in mobile DVB-T2 systems," *IEEE Transactions Broadcasting*, vol.57, no.3, pp.617-628, Sep.2011. Article (CrossRef Link).

[6] H. G. Yeh, Y. K. Chang and B. Hassibi, "A scheme for cancelling intercarrier interference using conjugate transmission in multicarrier communication systems," *IEEE Transactions Wireless Commun*ication, vol.6, no.1, pp.3-7, Jan.2007. Article (CrossRef Link).

[7] Y. Mostofi and D. Cox, "ICI mitigation for pilot-aided OFDM mobile systems," *IEEE Transactions Wireless Communication*, vol.4, no.2, pp.765-774, Mar.2005. Article (CrossRef Link).

[8] X. ma, G. B. Giannakis and S. Ohno, "Optimal training for block transmissions over doubly selective wireless fading channels," *IEEE Transactions Signal Processing*, vol.51, no.5, pp.1351-1366, May.2003. Article (CrossRef Link).

[9] G. Leus, "On the estimation of rapidly time-varying channels," in *Proc. of European Signal Process. Conf.*, vol. 4, pp. 2227-2230, Sep. 2004. Article (CrossRef Link).

[10] T. Zemen and C. F. Mecklenbrauker, "Time-variant channel estimation using discrete prolate spheroidal sequences," *IEEE Transactions Signal Processing*, vol.53, no.9, pp.3597-3607, Sep.2005. Article (CrossRef Link).

Seo Weon Heo received the B.S. and M.S. degrees in electronic engineering from Seoul National University, Korea in 1990 and 1992, respectively, and the Ph.D. degree in electrical engineering from the Purdue University, West Lafayette, Indiana, in 2001. From 1992 to1998, he was with the Digital Media Research Laboratory, LG Electronics Co., Ltd., Korea. From 2001 to 2006, he worked at the Telecommunication R&D Center, Samsung Electronics Co., Ltd., Korea. Since 2006, he has been an Associate professor with the School of Electronic and Electrical Engineering, Hongik University, Seoul, Korea. His current research interests are in the area of wireless communication, channel coding, embedded system HW/SW design.

Jongtae Lim received the B.S. (summa cum laude) and M.S. degrees in Electronics Engineering from Seoul National University, Seoul, Korea in 1989 and 1991, respectively, and received the Ph.D. degree from the Department of Electrical Engineering and Computer Science, University of Michigan, Ann Arbor, in 2001. In September 2004, he joined Korea Aerospace University, Goyang, Korea. Since March 2008, he has been with Hongik University, Seoul, Korea, where he is now Associate Professor of the School of Electronic & Electrical Engineering. His research and teaching interest are in digital communications, broadcasting systems and signal processing.